

# Determination of absolute photoionization cross sections for isomers of $C_3H_5$ : allyl and 2-propenyl radicals

Jason C. Robinson<sup>a,b,1</sup>, Niels E. Sveum<sup>a,b</sup>, Daniel M. Neumark<sup>a,b,\*</sup>

<sup>a</sup> Department of Chemistry, University of California, Berkeley, CA 94720, USA

<sup>b</sup> Chemical Sciences Division, Lawrence Berkeley National Laboratory, Berkeley, CA 94720, USA

Received 9 October 2003; in final form 4 November 2003

## Abstract

The photoionization (PI) cross sections of allyl and 2-propenyl radicals to form  $C_3H_5^+$  were measured using tunable vacuum ultraviolet (VUV) synchrotron radiation coupled with photofragment translational spectroscopy. At 10 eV, the cross sections were found to be  $6.2 \pm 1.2$  and  $5.1 \pm 1.0$  Mb, respectively. Using these values, the PI efficiency curves for each radical were placed on an absolute scale from 7.75 to 10.75 eV.

© 2003 Elsevier B.V. All rights reserved.

## 1. Introduction

There has been a substantial expansion of the role of tunable synchrotron radiation and vacuum ultraviolet (VUV) lasers in physical chemistry experiments, ranging from photodissociation and molecular beam scattering experiments to flame diagnostics [1–7]. In these experiments, VUV radiation is used to photoionize reaction or photo-products, which are subsequently mass-selected and detected. Photoionization (PI) results in substantially less fragmentation than in earlier detection schemes based on electron impact ionization, thereby facilitating product identification and characterization. However, extraction of information such as product branching ratios from this new class of experiments requires PI cross sections for each chemical species probed. While PI cross sections for many closed shell molecules have been determined [8], the determination of these cross sections for free radicals is quite challenging, as it is usually not feasible to generate known concentrations of these species.

We have recently demonstrated a general method for obtaining absolute PI cross sections for radicals [9], in which photofragment translational spectroscopy (PTS) is coupled with tunable VUV–PI of momentum-matched photofragments, one of which has a known PI cross section. One can then determine the PI cross section of the other fragment, even if the system exhibits complex photodissociation dynamics. This method was previously applied to the vinyl ( $C_2H_3$ ) and propargyl ( $C_3H_3$ ) radicals via photodissociation of vinyl and propargyl chloride. In this Letter, we investigate two isomers of the  $C_3H_5$  radical, allyl ( $CH_2CHCH_2$ ) and 2-propenyl ( $CH_2CCH_3$ ), produced by 193 nm photolysis of allyl chloride and 2-chloropropene, respectively, and determine their absolute PI cross sections using the known PI cross section for atomic chlorine [8,10–13].

Butler and co-workers [14] studied the photodissociation dynamics of allyl chloride and 2-chloropropene [2,15] at 193 nm using PTS coupled with tunable VUV synchrotron radiation to determine primary and secondary decomposition channels for each species. Fig. 1 presents an energy level diagram for Cl loss from allyl chloride and 2-chloropropene at 193 nm, using NIST thermochemical data [16] to establish the location of allyl+Cl and 2-chloropropene with respect to allyl chloride. The remaining reaction energetics, including

\* Corresponding author. Fax: +1-510-642-3635.

E-mail address: [dan@radon.cchem.berkeley.edu](mailto:dan@radon.cchem.berkeley.edu) (D.M. Neumark).

<sup>1</sup> Intel Corporation, Hillsboro, OR 97124.

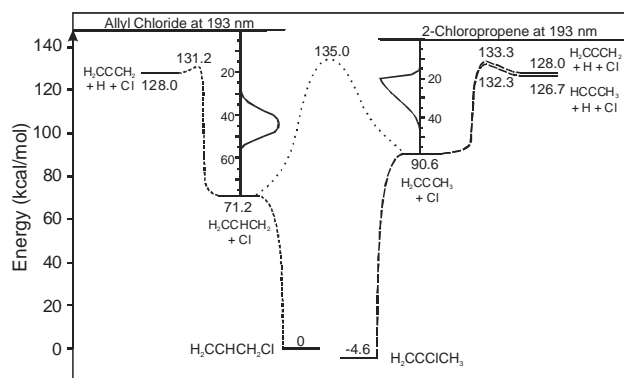


Fig. 1. Energy level diagram for 193 nm photodissociation of allyl chloride (left-hand side) and 2-chloropropene (right-hand side).

barrier heights to isomerization and decomposition of the nascent  $\text{C}_3\text{H}_5$  photoproducts, are referenced to the allyl+Cl channel. These energetics come from G2 (B3LYP) calculations of the  $\text{C}_3\text{H}_5$  potential energy surface by Davis et al. [17], which match those found by Wang et al. [18]. Fig. 1 shows that, in addition to Cl loss, secondary dissociation of  $\text{C}_3\text{H}_5$  to yield  $\text{C}_3\text{H}_4 + \text{H}$  is energetically accessible; this process occurs to an appreciable extent only for 2-chloropropene [2,15]. The barrier to dissociation of  $\text{C}_3\text{H}_5$  to  $\text{C}_3\text{H}_3 + \text{H}_2$  (not shown) was calculated to be 6.7 kcal/mol higher than the barrier to propyne + H [18], so this secondary dissociation process is unlikely to be significant. In any case, our analysis scheme based on momentum-matched fragments allows us to extract PI cross sections for the  $\text{C}_3\text{H}_5$  radicals even in the presence of extensive secondary dissociation.

## 2. Experiment

The experiments described in this Letter were performed using a rotating-source/fixed-detector crossed molecular beams instrument located on the Chemical Dynamics Beamline at the Advanced Light Source [1]. Briefly, a pulsed valve (100 Hz, 0.5 mm diameter nozzle, 200–300 Torr,  $\sim 80^\circ\text{C}$ ) was used to generate a molecular beam of either  $\sim 2\%$  allyl chloride (99%, Aldrich) or 2-chloropropene (98%, Aldrich) in helium. The molecular beam was skimmed and crossed by a 193 nm ArF excimer laser beam propagating orthogonally to both the molecular beam and detector axes. Laser power was controlled to minimize multiphoton processes.

Scattered photofragments entering the detector travelled 15.1 cm prior to ionization by tunable VUV synchrotron radiation, mass-selection by a quadrupole mass filter, and counting as a function of time with a multichannel scaler, producing angle-resolved TOF spectra for ions with a specific mass-to-charge ratio ( $m/e$ ). Data were collected with a multichannel scaler bin width of 1  $\mu\text{s}$  and rebinned to 2  $\mu\text{s}$ . The properties of

the VUV radiation have been described elsewhere [19–21]; the energy resolution ( $\Delta E/E$ ) was 2.3%. A rare gas filter was used to remove the higher harmonics of the undulator radiation [19], and a  $\text{MgF}_2$  window was placed in the path of the undulator radiation for PI energies below 10.8 eV to mitigate the effects of any residual high energy tail on the fundamental.

As described in our earlier work [9], two types of photodissociation measurements were performed. First, to determine a center-of-mass (CM) frame translational energy distribution ( $P(E_T)$  distribution) for each process, we collected a set of laboratory frame TOF spectra for each pair of momentum-matched photofragments. Second, by fixing the laboratory angle ( $\Theta_{\text{LAB}}$ ) and  $m/e$ , then stepping the undulator radiation, a series of TOF spectra was obtained. Integration of this series of measurements (following normalization by VUV photon flux, laser shots, laser power, etc.) yields a photoionization efficiency (PIE) curve, showing relative PI cross section as a function of photon energy. Through analysis of the TOF measurements, absolute PI cross sections were determined and used to place these PIE curves on an absolute scale.

## 3. Results and analysis

### 3.1. TOF Spectra

Fig. 2 presents representative TOF spectra for atomic chlorine ( $m/e = 35$ ) and allyl radical ( $m/e = 41$ ) produced by 193 nm photodissociation of allyl chloride, while Fig. 3 shows TOF spectra for atomic chlorine and 2-propenyl radical ( $m/e = 41$ ) from 2-chloropropene. For purposes of comparison, the TOF signal for the polyatomic fragment has been normalized to that of the atomic chlorine for each angle. The PI energies used were 10.0 eV for the  $\text{C}_3\text{H}_5$  radical and 15.0 eV for Cl atom; additional TOF spectra were acquired at various laboratory angles between  $10^\circ$  and  $60^\circ$ . Except for the normalization, these TOF spectra are similar to those reported by Butler and co-workers [2,14,15,22].

### 3.2. Translational energy distributions

The  $P(E_T)$  distributions shown in Fig. 4a and b (and inset in Fig. 1) were used to fit the TOF spectra presented in Figs. 2 and 3, respectively; each fit was obtained by forward convolution of the  $P(E_T)$  distribution with various parameters that characterize the instrument [23,24]. The  $P(E_T)$  distributions were adjusted point-wise until the simulations simultaneously fit the TOF spectra at all observed angles.

For allyl chloride, the fit to the  $m/e = 35$  TOF spectra shows the contribution that is momentum-matched to the  $m/e = 41$  signal. These fragments are

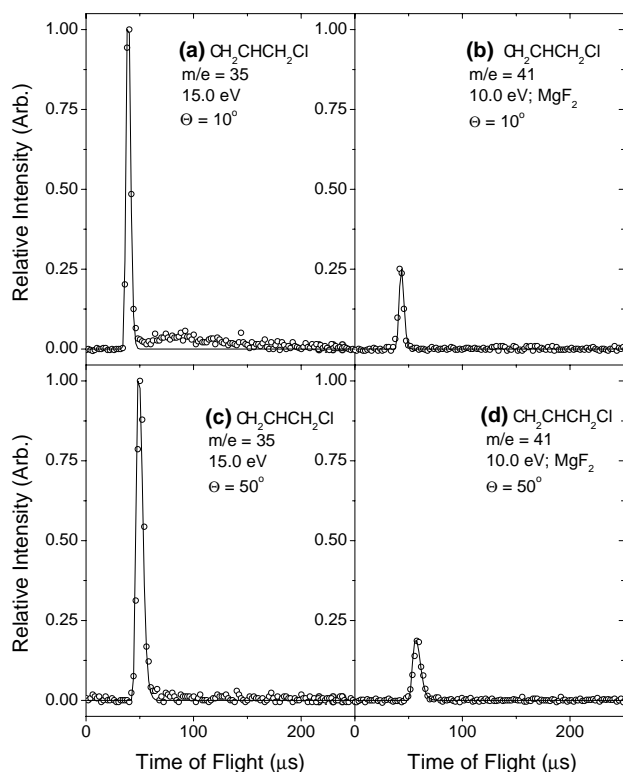


Fig. 2. TOF spectra from allyl chloride dissociation: (a)  $m/e = 35$  ( $\text{Cl}^+$ ) and (b)  $m/e = 41$  ( $\text{C}_3\text{H}_5^+$ ) at  $\theta_{\text{LAB}} = 10^\circ$ ; and (c)  $m/e = 35$  and (d)  $m/e = 41$  at  $\theta_{\text{LAB}} = 50^\circ$ . TOF signal has been normalized for laser shots, laser power, VUV photon flux, and isotopic abundance. The polyatomic fragment signal has been normalized with respect to the chlorine signal for each angle. Open circles represent the data and the solid line represents the fit using the appropriate  $P(E_T)$  distribution from Fig. 4.

attributed to excited state dissociation [14]. The additional slow features in the  $m/e = 35$  TOF spectra were suggested by Morton et al. [14] to result from internal conversion prior to chlorine loss on the ground state. Similarly,  $m/e = 35$  TOF spectra for 2-chloropropene include additional slower components, assigned by Mueller et al. [2,15] as two separate channels that form  $\text{Cl} + \text{H} + \text{C}_3\text{H}_4$  through secondary decomposition of the nascent  $\text{C}_3\text{H}_5$  product. The  $P(E_T)$  distribution for the momentum-matched  $\text{Cl}$  and  $\text{C}_3\text{H}_5$  products in Fig. 4b supports this assignment. This distribution is truncated below  $E_T = 20$  kcal/mol; as seen in Fig. 1, lower values of  $E_T$  correspond to internal energies in the  $\text{C}_3\text{H}_5$  that exceed the barrier for decomposition to  $\text{C}_3\text{H}_4 + \text{H}$ . For purposes of obtaining the absolute PI cross sections of the  $\text{C}_3\text{H}_5$  isomers, only the momentum-matched component of the  $m/e = 35$  TOF data is of interest.

### 3.3. Absolute photoionization cross sections and photoionization efficiency curves for $\text{C}_3\text{H}_5$ radicals

Using the  $P(E_T)$  distributions in Fig. 4, a set of TOF spectra for the momentum-matched fragments can be fit

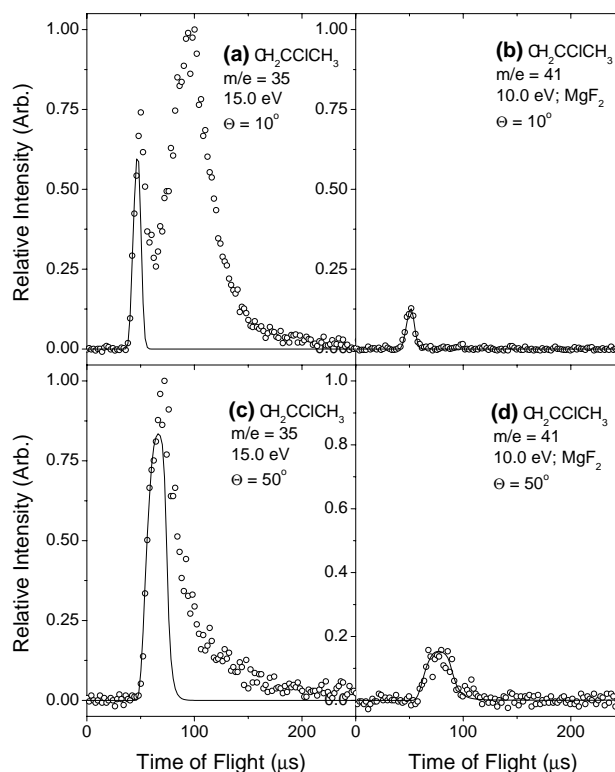


Fig. 3. TOF spectra from 2-chloropropene dissociation: (a)  $m/e = 35$  ( $\text{Cl}^+$ ) and (b)  $m/e = 41$  ( $\text{C}_3\text{H}_5^+$ ) at  $\theta_{\text{LAB}} = 10^\circ$ ; and (c)  $m/e = 35$  and (d)  $m/e = 41$  at  $\theta_{\text{LAB}} = 50^\circ$ .

to yield scaling factors that normalize the TOF spectra produced through forward convolution. Essentially, these scaling factors represent the ratio of weighting factors necessary for convolution of the  $P(E_T)$  distribution to reproduce observed lab frame TOF intensities; this analysis accounts for all kinematic effects. For  $\text{C}_3\text{H}_5\text{Cl} + h\nu_{193\text{ nm}} \rightarrow \text{C}_3\text{H}_5 + \text{Cl}$ , one obtains the relative cross section for the momentum-matched photofragments at specified PI energies, i.e.,  $\sigma_{\text{C}_3\text{H}_5}(10\text{ eV})/\sigma_{\text{Cl}}(15\text{ eV})$ , which has been normalized for experimental conditions such as laser power, number of laser shots, VUV photon flux, and isotopic abundance (data were taken only at  $m/e = 35$  for chlorine). No correction for relative transmission through the quadrupole mass spectrometer was included, because the ion masses are similar and this correction has been found to be small [4].

The photon energy of 15.0 eV is centered in a relatively flat region of the Cl photoionization spectrum, as shown by Ruscic and Berkowitz [10]. As discussed previously [9], we take the value of the absolute PI cross section for Cl to be  $\sigma_{\text{Cl}} = 27.3$  Mb at 15.0 eV, based on the recommendation by Berkowitz [8] of 34.2 Mb for the  $\text{Cl}^+(^1\text{S})$  edge in the PI spectrum of Cl. From this value of  $\sigma_{\text{Cl}}$ , we find  $\sigma_{\text{C}_3\text{H}_5, \text{allyl}} = 6.2$  Mb and  $\sigma_{\text{C}_3\text{H}_5, 2\text{-propenyl}} = 5.1$  Mb at 10.0 eV, with estimated error bars of  $\pm 20\%$ . Using these cross sections, PIE curves for the  $\text{C}_3\text{H}_5$  products were placed on an absolute scale, as shown in Fig. 5.

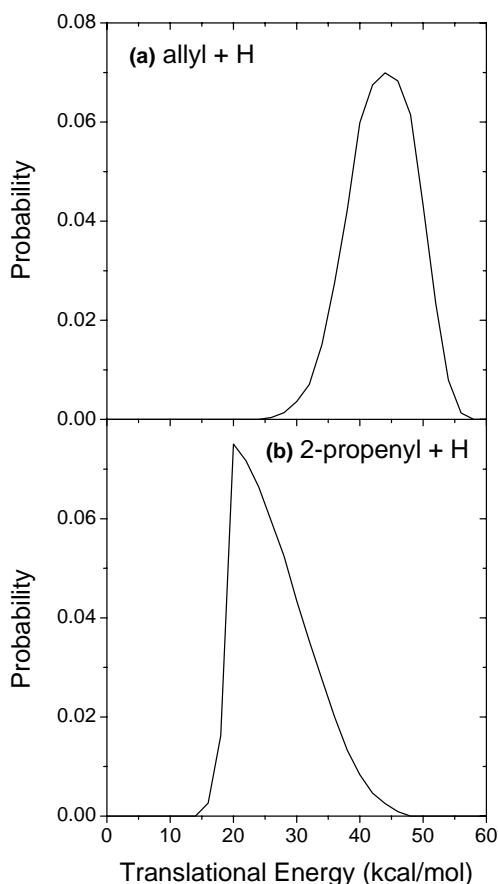


Fig. 4.  $P(E_T)$  distributions for  $C_3H_5 + Cl$  from (a) allyl chloride and (b) 2-chloropropene.

#### 4. Discussion

Due to the complex nature of  $C_3H_5Cl$  photodissociation, several factors could affect the accuracy and interpretation of the absolute PI cross sections obtained from these experiments, including possible isomerization, internal excitation, and dissociative ionization (DI) of  $C_3H_5$  photofragments. Each of these points will be considered below.

First, one would like to ascertain that the  $m/e = 41$  products from the two precursors are two distinct  $C_3H_5$  isomers, namely the allyl (3-propenyl) and 2-propenyl radicals. By inspection of the TOF spectra and forward convolution fits presented here and by others [2,14,15,22], it is clear that the 193 nm Cl loss dynamics for allyl chloride and 2-chloropropene are distinct processes. Moreover, the PIE curves in Fig. 5 are similar but not identical, suggesting that the detected  $C_3H_5$  products are different species, and that scrambling between  $C_3H_5$  isomers subsequent to C–Cl bond cleavage but prior to ionization does not occur.

Separate G2(B3LYP) [17] and G3(B3LYP) [18] calculations of the  $C_3H_5$  potential energy surface, which agree to within 1 kcal/mol, yield isomerization barriers

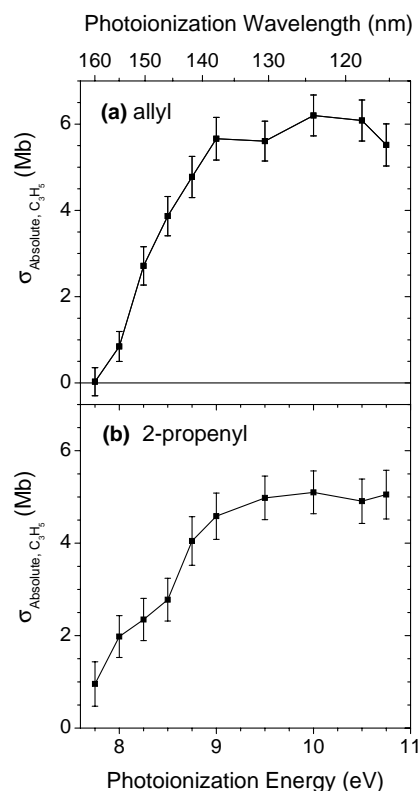


Fig. 5. PIE curve for  $m/e = 41$  ( $C_3H_5^+$ ) photoproduct at  $\theta_{LAB} = 30^\circ$  from (a) allyl chloride and (b) 2-chloropropene, using the  $MgF_2$  window. The solid squares represent the data points with  $2\sigma$  error bars.

between allyl, 2-propenyl, and 1-propenyl radicals. The lowest of these barriers is between allyl and 2-propenyl radicals; this barrier, shown in Fig. 1, lies 135 kcal/mol above allyl chloride barrier to isomerization is between allyl and 2-propenyl radicals, at 135 kcal/mol with respect to allyl chloride. The inset  $P(E_T)$  distributions indicate the amount of internal energy remaining in the fragments relative to isomerization and decomposition barriers. The allyl radical from allyl chloride does not have sufficient internal energy to surmount these barriers. The 2-propenyl radical from 2-chloropropene has more internal energy, but, as shown in Fig. 1, the cutoff at low  $E_T$  for the  $C_3H_5$  product from photodissociation of 2-chloropropene distribution agrees well with the calculated dissociation barriers for H-atom loss from 2-propenyl. These barriers are slightly lower than that for isomerization to allyl and will correspond to significantly looser transition states. Hence, isomerization should not be competitive with H-atom loss for even the most highly excited 2-propenyl products. We thus believe that our cross sections and PIE curves correspond to isomerically distinct  $C_3H_5$  species.

We next consider how the internal energy of the  $C_3H_5$  products affects the PI cross sections. Because no collisions occur after photolysis, the nascent internal energy distribution of the polyatomic fragments does not relax prior to ionization. For the case of allyl, the most

probable value for translational energy is 44 kcal/mol (Fig. 4a), leaving 33 kcal/mol available for internal excitation of the  $C_3H_5$  fragment; for 2-propenyl,  $E_T = 22$  kcal/mol leaves 30 kcal/mol available [16,25]. For  $C_3H_5$ , the internal energy can be distributed into  $n = 18$  vibrational degrees of freedom, corresponding to  $T \sim 920$  K for allyl and  $T \sim 840$  K for 2-propenyl. As a result, ion signal is observed in Fig. 5a at photon energies below the ionization potential of allyl, previously found to be 8.153 eV by ZEKE spectroscopy [26]. This excitation can affect the value of the PI cross section just above the ionization threshold by shifting of the PIE curve toward lower energy [9]; the extent to which this occurs depends on the Franck–Condon factors for ionization. However, for both isomers, the PIE curves are flat around 10 eV, so our reported values of the PI cross sections at that energy are unlikely to be affected significantly by internal excitation.

Finally, one must recognize that the cross sections reported here are for production of  $C_3H_5^+$  only and do not include DI. Dissociative Ionization can occur over the range of photon energies used in this investigation. For example, recent threshold-photoelectron photoion coincidence (TPEPICO) studies of the allyl radical [27] indicate that above 10.0 eV, allyl undergoes some DI to produce  $C_3H_3^+$ . Butler and co-workers [2,14] also observed evidence for DI of  $C_3H_5$  to  $C_3H_3^+$  at PI energies around 11 eV. Hence, our cross sections are partial PI cross sections for parent ion production rather than total cross sections; future measurements of relative PIE curves for parent versus fragment ion formation will allow total PI cross sections to be determined from the results presented here. Nonetheless, the partial cross sections reported here are the values required to determine, for example, the number density of  $C_3H_5$  radicals associated with a measured  $C_3H_5^+$  photoion signal.

## 5. Conclusions

PTS has been coupled with VUV–PI detection to determine the PI cross sections for allyl and 2-propenyl radicals. Although the 193 nm photodissociation dynamics of the precursors, allyl chloride and 2-chloropropene, are quite complex, we can extract the relevant PI cross sections by fitting momentum-matched TOF data from the Cl and  $C_3H_5$  fragments. At 10 eV, we find these cross sections to be  $\sigma_{C_3H_5,allyl} = 6.2$  Mb and  $\sigma_{C_3H_5,2-propenyl} = 5.1$  Mb, with estimated error bars of  $\pm 20\%$ , and use these values to place the PIE curves for ionization of these two  $C_3H_5$  isomers to  $C_3H_5^+$  on an absolute scale from 7.75 to 10.75 eV. The cross sections at 10 eV are smaller than those for vinyl and propargyl radicals, 11.1 and 8.3 Mb, respectively [9], possibly reflecting more DI for the two  $C_3H_5$  radicals.

## Acknowledgements

This work was supported by the Director, Office of Basic Energy Sciences, Chemical Sciences Division of the US Department of Energy under contract No. DE AC03-76SF00098.

## References

- [1] X. Yang, D.A. Blank, J. Lin, A.M. Wodtke, A.G. Suits, Y.T. Lee, *Rev. Sci. Instrum.* 68 (1997) 3317.
- [2] J.A. Mueller, B.F. Parsons, L.J. Butler, F. Qi, O. Sorkhabi, A.G. Suits, *J. Chem. Phys.* 114 (2001) 4505.
- [3] J.C. Robinson, W. Sun, S.A. Harris, F. Qi, D.M. Neumark, *J. Chem. Phys.* 115 (2001) 8359.
- [4] J.C. Robinson, S.A. Harris, W. Sun, N.E. Sveum, D.M. Neumark, *J. Am. Chem. Soc.* 124 (2002) 10211.
- [5] W.S. McGivern, O. Sorkhabi, A.G. Suits, A. Derecskei-Kovacs, S.W. North, *J. Phys. Chem.* 104 (2000) 10085.
- [6] C.Y. Ng, *Ann. Rev. Phys. Chem.* 53 (2002) 101.
- [7] T.A. Cool, T.A. Mostefaoui, F. Qi, A. McIlroy, P.R. Westmoreland, M.E. Law, L. Poisson, D.S. Peterka, M. Ahmed, *J. Chem. Phys.* 119 (2003) 8356.
- [8] J. Berkowitz, *Atomic and Molecular Photoabsorption: Absolute Total Cross Sections*, Academic Press, San Diego, CA, 2002.
- [9] J.C. Robinson, N.E. Sveum, D.M. Neumark, *J. Chem. Phys.* 119 (2003) 5311.
- [10] B. Ruscic, J. Berkowitz, *Phys. Rev. Lett.* 50 (1983) 675.
- [11] J.A.R. Samson, Y. Shefer, G.C. Angel, *Phys. Rev. Lett.* 56 (1986) 2020.
- [12] W.J. van der Meer, R.J. Butselaar, C.A. de Lange, *Aust. J. Phys.* 39 (1986) 779.
- [13] R. Flesch, J. Plenge, S. Kuhl, M. Klusmann, E. Ruhl, *J. Chem. Phys.* 117 (2002) 9663.
- [14] M.L. Morton, L.J. Butler, T.A. Stephenson, F. Qi, *J. Chem. Phys.* 116 (2002) 2763.
- [15] J.A. Mueller, J.L. Miller, L.J. Butler, F. Qi, O. Sorkhabi, A.G. Suits, *J. Phys. Chem. A* 104 (2000) 11261.
- [16] P.J. Linstrom, W.G. Mallard (Eds.), *NIST Chemistry Webbook, NIST Standard Reference Database Number 69*. National Institute of Standards and Technology, Gaithersburg, MD, 2003.
- [17] S.G. Davis, C.K. Law, H. Wang, *J. Phys. Chem. A* 103 (1999) 5889.
- [18] B. Wang, H. Hou, Y. Gu, *J. Chem. Phys.* 112 (2000) 8458.
- [19] A.G. Suits, P. Heimann, X.M. Yang, M. Evans, C.W. Hsu, K.T. Lu, Y.T. Lee, A.H. Kung, *Rev. Sci. Instrum.* 66 (1995) 4841.
- [20] M. Koike, P.A. Heimann, A.H. Kung, T. Namioka, R. Digenaro, B. Gee, N. Yu, *Nucl. Instrum. Meth. Phys. Res. A* 347 (1994) 282.
- [21] P.A. Heimann, M. Koike, C.W. Hsu, M. Evans, C.Y. Ng, D. Blank, X.M. Yang, C. Flaim, A.G. Suits, Y.T. Lee, *SPIE Proc.* 2856 (1996) 90.
- [22] T.L. Myers, D.C. Kitchen, B. Hu, L.J. Butler, *J. Chem. Phys.* 104 (1996) 5446.
- [23] X. Zhao, *Photodissociation of cyclic compounds in a molecular beam*, PhD Thesis, University of California, Berkeley, CA, 1988.
- [24] J.D. Myers, *Chemical dynamics in time and energy space*, PhD Thesis, University of California, Berkeley, CA, 1993.
- [25] J.A. Miller, C.F. Melius, *Combust. Flame* 91 (1992) 21.
- [26] T. Gilbert, I. Fischer, P. Chen, *J. Chem. Phys.* 113 (2000) 561.
- [27] T. Schuessler, H.-J. Deyerl, S. Duemmler, I. Fischer, C. Alcaraz, M. Elhanine, *J. Chem. Phys.* 118 (2003) 9077.